Metal–Organic Frameworks

DOI: 10.1002/ange.200600976

Metastable Sorption State of a Metal–Organic Porous Material Determined by In Situ Synchrotron Powder Diffraction**

Yoshiki Kubota, Masaki Takata, Ryotaro Matsuda, Ryo Kitaura, Susumu Kitagawa, and Tatsuo C. Kobayashi*

Metal–organic microporous materials (MOMMs)[1] have attracted the attention of scientists for a number of reasons including the creation of nanometer-sized spaces, discovery of novel phenomena, and commercial interests such as their application in gas separation,[2] gas storage,[2,3] and heterogeneous catalysis.[4] Recent activity in crystal engineering has provided several examples of MOMMs which have rigid open frameworks and therefore the potential to be functionally related to zeolites. In fact, MOMMs often have a much more dynamic framework than is generally believed, and this is

[*] Dr. Y. Kubota
Department of Physical Science
Graduate School of Science
Osaka Prefecture University
Sakai, Osaka 590-0035 (Japan)
Fax: (+81) 72-222-4791
E-mail: kubotay@p.s.osakafu-u.ac.jp
Dr. M. Takata[+]
Japan Synchrotron Radiation Research Institute/SPring-8
Sayo-gun, Hyogo, 679-5198 (Japan)
and
CREST, Japan Science and Technology Agency (Japan)
Dr. R. Matsuda, Dr. R. Kitaura,[++] Prof. Dr. S. Kitagawa
Department of Synthetic Chemistry and Biological Chemistry
Graduate School of Engineering, Kyoto University
Katsura, Kyoto 615-8510 (Japan)
Prof. Dr. T. C. Kobayashi
Department of Physics
Okayama University
Okayama 700-8530 (Japan)
[+] Present address: Structural Materials Science Laboratory
Harima Institute, RIKEN SPring-8 Center
Sayo-gun, Hyogo, 679-5148 (Japan)
[++] Present address: Department of Chemistry
Graduate School of Sciences
Nagoya University
Nagoya 464-8603 (Japan)

[**] This study was supported by CREST/JST and JASRI/SPring-8 Nanotechnology Support Project of the Ministry of Education, Culture, Sports, Science and Technology of Japan. This study was also supported by a Grant-In-Aid for Science Research in a Priority Area "Chemistry of Coordination Space" from the Ministry of Education, Culture, Sports, Science and Technology of Japan. The authors thank Dr. K. Kato for the kind advice and support in data collection and Dr. H. Tanaka for the computer program ENIGMA for the MEM analysis.

Supporting information for this article is available on the WWW under http://www.angewandte.org or from the author.

characteristic of metal–organic species.[5] Dynamic pores could come from a sort of "soft" framework with multistability, whose states go back and forth between two counterparts; or a system could exist in one or two states for the same values of external field parameters. The structural rearrangement of the host framework in response to guest molecules proceeds from the "open" phase to the "closed" phase. The MOMMs could also be a unique class of materials with characteristics unlike those of rigid porous materials. While sorption profiles of MOMMs with saturated amounts of guests have been well characterized so far,[6] their intermediate profiles are still unknown. It is important to determine how guest molecules are recognized and finally confined by nanopores. An in-depth understanding of the intermediate state provides us with a feasible design for a porous framework which changes its structure into one well suited to a desired guest molecules and results in an efficient accommodation system. Therefore, fundamental structural information on not only the host framework but also the guest molecules is required throughout adsorption phenomena. X-ray diffraction is one of the most powerful methods that can directly provide structural information on the adsorbed molecules. Herein we report the structure analysis of an intermediate phase in the process of gas adsorption in the nanochannels of an MOMM by in situ synchrotron powder diffraction.

Previously,[2] we reported adsorption of acetylene gas on CPL-1 (coordination polymer 1 with pillared-layer structure: $Cu_2(pzdc)_2(pyz)$ where pzdc is pyrazine-2,3-dicarboxylate and pyz is pyrazine).[7] From accurate structural analysis, acetylene molecules were found to be trapped by forming double hydrogen bonds with uncoordinated carboxylate oxygen atoms. In situ powder diffraction patterns for gas adsorption between the anhydrous hollow phase (phase I) and the saturated adsorbed phase (phase S) revealed another phase mixed with phase S. It was also observed in the desorption process. The acetylene gas adsorption isotherm for CPL-1 at 270 K shows a steep rise in the very low pressure region and reaches saturation. During the rise, a step is evident at about 0.7 molecules per unit pore. These data suggest the existence of an intermediate phase of adsorption, which we call intermediate phase M. In the diffraction patterns for an acetylene gas pressure of 10 kPa reported previously,[2] phases S and M are mixed. By careful adjustment of both temperature and gas pressure, we succeeded in obtaining phase M as a single phase. Figure 1 shows the temperature dependence of the diffraction patterns of CPL-1 with acetylene under a constant gas pressure of 150 kPa. The sample was cooled from 390 K. The change in diffraction pattern at 360 K indicates that acetylene adsorption has started. Subsequently, another phase, assigned as phase S, appeared below 360 K. The peak intensities of phase M gradually decreased and those of phase S increased. The diffraction pattern at 360 K for single phase M was analyzed.

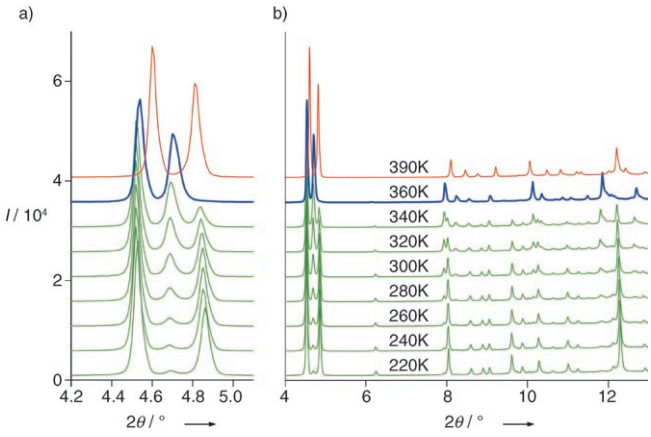

Figure 1. In situ synchrotron powder diffraction patterns of CPL-1 with adsorption of acetylene at 150 kPa. The 2θ ranges were a) from 4.2 to 5.1° and b) from 4.0 to 13.0°.

All the reflections were indexed with a monoclinic cell by the indexing program DICVOL91.[8] The lattice parameters were estimated to be $a = 11.3050$, $b = 20.2747$, $c = 4.7272$ Å, and $\beta = 98.669°$. The calculated figures of merit[9] were $M(20) = 12.7$, $F(20) = 57.4(0.0094, 37)$. These lattice parameters are very similar to those reported for CPL-1.[7] The structure was analyzed by the maximum entropy method (MEM)/Rietveld technique.[10] The MEM calculation was performed with the computer program ENIGMA.[11] The Rietveld refinement with soft constraints on bond lengths and angles was carried out by using $\sin\theta/\lambda = 0.45$ Å^{-1}. The final Rietveld fitting of phase M of CPL-1 with acetylene molecules at 150 kPa and 360 K shows a satisfactory fitting. The reliability (R) factors based on the powder profiles R_{WP} and the Bragg integrated intensities R_I were 3.27 and 4.70%, respectively. The fundamental structures of the CPL-1 frameworks of phases I, M, and S are all identical. The space group of these phases is $P2_1/c$. The effect of acetylene adsorption on the lattice parameters, unit cell volumes, and pore volumes of CPL-1 is shown in Table 1. Lattice parameters b, c, and β notably changed on acetylene adsorption. The unit cell of CPL-1 was found to expand once in phase M and contract to reach phase S, in which the acetylene molecules are trapped by forming double hydrogen bonds with oxygen atoms in the pore wall. On the other hand, the pore volume increased from phase I to M and was almost constant on going to phase S.

Table 1: Lattice parameters, unit cell volumes, and pore volumes of CPL-1. P is acetylene gas pressure, V_c is the unit cell volume, and V_p the pore volume.

Phase	P [kPa]	T [K]	a [Å]	b [Å]	c [Å]	β [°]	V_c [Å^3]	V_p [cm^3 g^{-1}]
Phase I[a]	0	390	4.7331(2)	19.9244(4)	10.8678(3)	96.009(4)	1019.25(5)	0.0876
Phase M	150	360	4.7094(1)	20.2467(5)	11.2824(4)	98.827(4)	1063.03(6)	0.104
Phase S[a]	10	170	4.81352(4)	20.2355(2)	10.7165(1)	96.937(1)	1036.18(3)	0.109
Phase I[b]	0	120	4.71534(6)	19.8280(2)	10.7184(1)	95.1031(10)	998.15(2)	0.0790

[a] From ref. [2]. [b] From ref. [6a].

Figure 2 shows the determined crystal structure of phase M of CPL-1 with adsorbed acetylene. Acetylene

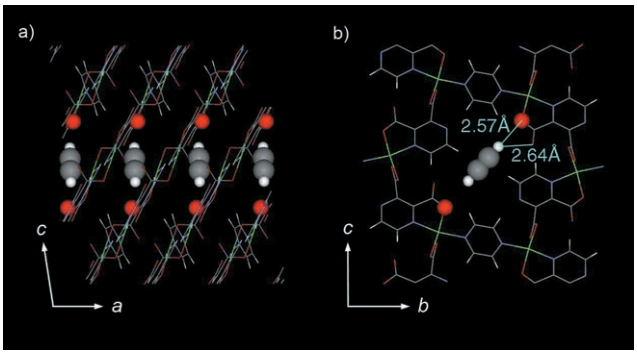

Figure 2. Determined crystal structure of phase M of CPL-1 with adsorbed acetylene. Views from a) side and b) front of the nanochannel directions. These figures show around one unit pore. Acetylene molecules (C gray, H white) and oxygen atoms (red; O1) of carboxylate bonded to the Cu ion are shown as spheres. Other atoms are connected by lines. Acetylene molecules occupy the sites with a probability of 0.7.

molecules are located in the center of the nanochannel with one molecular site per unit pore. The refined occupancy factor of the acetylene molecule was 0.70(2) and shows very good agreement with the step position in the adsorption isotherm. The isotropic thermal factor B of the acetylene molecule was refined to 17(3) Å^2. This large B value means that the adsorbed acetylene molecules have pronounced thermal motion. The molecular axis of acetylene is perpendicular to the nanochannel direction and is on the line connecting the two oxygen atoms O1 of carboxylate bonded to a Cu ion. This orientation is different from that in phase S, in which the molecular axis is on the line connecting the uncoordinated oxygen atoms O2 of carboxylate. The interatomic distance between the hydrogen atom of acetylene and the neighboring O1 atom is 2.57 Å, while the distance to the O2 atom is 2.64 Å. These values are approximately equal to the sum of the van der Waals radii of hydrogen (1.2 Å) and oxygen (1.4 Å), that is 2.6 Å. Figure 3 shows a section through

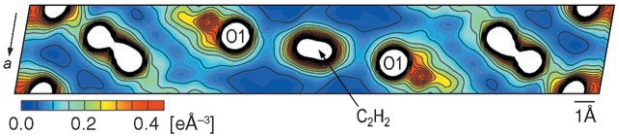

Figure 3. Section through the MEM charge density of phase M of CPL-1 with adsorbed acetylene. The section contains the molecular axis of acetylene and the a axis. Contour lines are drawn from 0.00 to 1.00 e Å^{-3} with intervals of 0.05 e Å^{-3}. Higher density regions are omitted.

the MEM charge density containing the molecular axis of acetylene. Little electron density was observed between the adsorbed acetylene molecules and O1 atoms. From these results, the interaction of acetylene molecules with the oxygen sites is much weaker in phase M than in phase S.

The assembled structures of rod-shaped molecules confined in CPL-1 indicate that the dimers align approximately parallel to the nanochannel direction.[6a,12] However, in the most stable arrangement in acetylene adsorption, the molecular axis of acetylene is perpendicular to the nanochannel direction in phase S. Since the size of an acetylene molecule is 5.5 × 3 Å and that of the rectangular nanochannel of CPL-1 is 4 × 6 Å, there is not enough space to permit acetylene molecules to adopt an orientation such as that allowed in phase S in the initial stage of adsorption. First, acetylene molecules are thought to be introduced into the nanochannels with their molecular axis along the nanochannel direction. Since the molecular size of 5.5 Å is larger than the lattice parameter a, which corresponds to the nanochannel direction in CPL-1, the adsorbed amount of molecules does not reach one molecule per unit pore and shows about 70% loading. After the introduction of acetylene molecules, they can easily rotate with thermal motion in the ac plane within the nanochannels. By this motion, they can align with the O1 atom for the first time within the restricted space of the nanochannel to form metastable phase M. Figure 4 shows

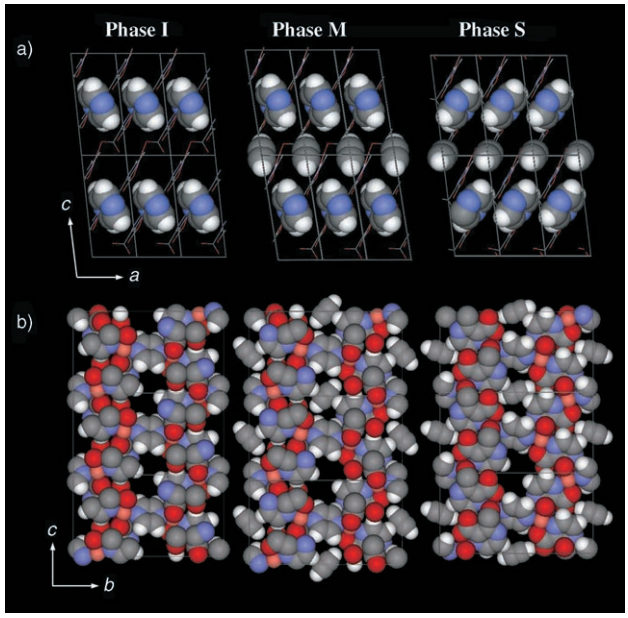

Figure 4. Crystal structures of CPL-1 with adsorped acetylene. a) Side views of the nanochannels. Pillar molecules (pyrazine) and adsorbed acetylene molecules are shown as CPK models. Otherwise, they are connected by lines. b) Views from the nanochannel direction as CPK model. Adsorbed acetylene molecules are omitted from lower central pore in phases M and S (C gray, H white, N blue, O red).

crystal structures of phases I, M, and S of CPL-1 with adsorption of acetylene. Slight rotation of the pillar ligands, that is, the pyrazine rings, and shearing of the crystal lattice in the a direction indicate flexible transformation for efficient guest accommodation. Subsequently, phase M changes to phase S with a slight rotation of acetylene molecules, and then hydrogen bonds are formed with the two uncoordinated oxygen atoms. With this change, there is now sufficient space for the pyrazine ring to rotate. The hydrogen bond between the hydrogen atom of pyrazine and the neighboring O1 atom is associated with rotation of the pyrazine rings. Their interatomic distance is 2.3 Å in phase S. This results in rather a different orientation of pyrazine in phase S from

that in phases I and M. Shearing of the lattice also occurs again to permit more efficient guest accommodation. In the phase change from phase M to S, the unit cell volume decreases, whereby the lattice parameter *c* contracts due to the change in orientation of the acetylene molecule forming double hydrogen bonds with two oxygen atoms on the pore wall. However, rotation of the pillar ligand makes space without changing the pore volume significantly. At the same time, the change in size and shape of the nanochannel causes more acetylene loading to reach saturation of adsorption. This process is schematically shown in Figure 5.

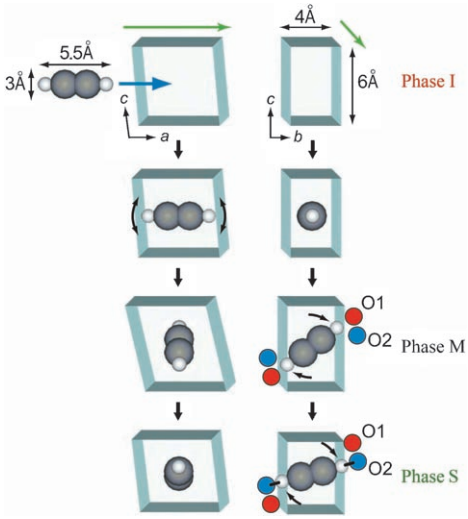

Figure 5. Schematic illustration of the adsorption process of acetylene in the nanochannel of CPL-1. Views from the side (left) and front (right) of the nanochannel directions. Boxes show the rectangular nanochannels. Green arrows show the nanochannel direction. Blue and red filled circles indicate the oxygen atoms of carboxylate. C gray, H white.

Phase M is the metastable state in the process. The molecular orientation changes within the restricted space in the nanochannel to reach the saturated adsorbed phase S. The CPL-1 framework expands once in phase M and contracts to reach phase S. Then rotation of the pillar ligands and lattice shearing occur to permit efficient guest accommodation. Using X-ray structure analysis, we have succeeded in visualizing the rearrangement of guest molecules and the transformation of the framework in the process of adsorption. We also found that the flexible framework of MOMMs can vary not only with guest size and/or shape but also with the amount of guest molecules to form optimum structures for guest accommodation. These findings will contribute to the development of novel functional MOMMs responsive to guest molecules. More structural studies on the gas adsorption process should be performed to attain an in-depth understanding of the adsorption phenomena.

Experimental Section

The synthesis and fundamental crystal structure of CPL-1 were reported previously.[7] The in situ synchrotron powder diffraction experiment was carried out at BL02B2 SPring-8 with a large Debye–Scherrer type diffractometer[13] equipped with a gas handling system. The wavelength of the incident X rays was 0.801 Å. The powder sample was loaded into a soda glass capillary with 0.4-mm inner diameter. The temperature was controlled by a low-temperature nitrogen gas blower. Before the measurements, the sample was heated to 390 K for 15 min in vacuum to remove water molecules present in the nanochannels. The diffraction pattern at 390 K was confirmed to be that of the anhydrous hollow phase of CPL-1. After that, acetylene gas was dosed into the capillary sample through a stainless steel tube. The amount of gas adsorption was controlled by changing the sample temperature under constant gas pressure. The exposure time of each temperature point was 5 min, and 10 min intervals were maintained before measurements so as to reach the equilibrium adsorption state. CCDC 294513 contains the supplementary crystallographic data for this paper. These data can be obtained free of charge from The Cambridge Crystallographic Data Centre via www.ccdc.cam.ac.uk/data_request/cif.

Received: March 13, 2006
Revised: April 28, 2006
Published online: June 29, 2006

Keywords: adsorption · metal–organic frameworks · microporous materials · structure elucidation · X-ray diffraction

[1] a) O. M. Yaghi, M. O'Keeffe, N. W. Ockwig, H. K. Chae, M. Eddaoudi, J. Kim, *Nature* **2003**, *423*, 705–714; b) S. Kitagawa, R. Kitaura, S. Noro, *Angew. Chem.* **2004**, *116*, 2388–2430; *Angew. Chem. Int. Ed.* **2004**, *43*, 2334–2375.
[2] R. Matsuda, R. Kitaura, S. Kitagawa, Y. Kubota, R. V. Belosludov, T. C. Kobayashi, H. Sakamoto, T. Chiba, M. Takata, Y. Kawazoe, Y. Mita, *Nature* **2005**, *436*, 238–241.
[3] a) S. Noro, S. Kitagawa, M. Kondo, K. Seki, *Angew. Chem.* **2000**, *112*, 2161–2164; *Angew. Chem. Int. Ed.* **2000**, *39*, 2082–2084; b) K. Seki, W. Mori, *J. Phys. Chem. B* **2002**, *106*, 1380–1385; c) G. Férey, M. Latroche, C. Serre, F. Millange, T. Loiseau, A. Percheron-Guégan, *Chem. Commun.* **2003**, *24*, 2976–2977; d) D. N. Dybtsev, H. Chun, S. H. Yoon, D. Kim, K. Kim, *J. Am. Chem. Soc.* **2004**, *126*, 32–33; e) J. L. C. Rowsell, A. R. Millward, K. S. Park, O. M. Yaghi, *J. Am. Chem. Soc.* **2004**, *126*, 5666–5667.
[4] a) O. Ohmori, M. Fujita, *Chem. Commun.* **2004**, 1586–1587; b) J. S. Seo, D. Whang, H. Lee, S. I. Jun, J. Oh, Y. J. Jeon, K. Kim, *Nature* **2000**, *404*, 982–986.
[5] a) R. Matsuda, R. Kitaura, S. Kitagawa, Y. Kubota, T. C. Kobayashi, S. Horike, M. Takata, *J. Am. Chem. Soc.* **2004**, *126*, 14063–14070; b) D. N. Dybtsev, H. Chun, K. Kim, *Angew. Chem.* **2004**, *116*, 5143–5146; *Angew. Chem. Int. Ed.* **2004**, *43*, 5033–5036.
[6] a) R. Kitaura, S. Kitagawa, Y. Kubota, T. C. Kobayashi, K. Kindo, Y. Mita, A. Matsuo, M. Kobayashi, H. Chang, T. C. Ozawa, M. Suzuki, M. Sakata, M. Takata, *Science* **2002**, *298*, 2358–2361; b) Y. Kubota, M. Takata, R. Matsuda, R. Kitaura, S. Kitagawa, K. Kato, M. Sakata, T. C. Kobayashi, *Angew. Chem.* **2005**, *117*, 942–945; *Angew. Chem. Int. Ed.* **2005**, *44*, 920–923; c) S. Takamizawa, E. Nakata, *CrystEngComm* **2005**, *7*, 476–479; d) G. J. Halder, C. J. Kepert, *J. Am. Chem. Soc.* **2005**, *127*, 7891–7900; e) J. L. C. Rowsell, E. C. Spencer, J. Eckert, J. A. Howard, O. M. Yaghi, *Science* **2005**, *309*, 1350–1354.
[7] M. Kondo, T. Okubo, A. Asami, S. Noro, T. Yoshitomi, S. Kitagawa, T. Ishii, H. Matsuzaka, K. Seki, *Angew. Chem.* **1999**, *111*, 190–193; *Angew. Chem. Int. Ed.* **1999**, *38*, 140–143.
[8] A. Boultif, D. Louer, *J. Appl. Crystallogr.* **1991**, *24*, 987–993.
[9] a) P. M. de Wolff, *J. Appl. Crystallogr.* **1968**, *1*, 108–113; b) G. S. Smith, R. L. Snyder, *J. Appl. Crystallogr.* **1979**, *12*, 60–65.

[10] a) M. Takata, B. Umeda, E. Nishibori, M. Sakata, Y. Saito, M. Ohno, H. Shinohara, *Nature* **1995**, *377*, 46 – 49; b) M. Takata, E. Nishibori, M. Sakata, *Z. Kristallogr.* **2001**, *216*, 71 – 86.
[11] H. Tanaka, M. Takata, E. Nishibori, K. Kato, T. Iishi, M. Sakata, *J. Appl. Crystallogr.* **2002**, *35*, 282 – 286.
[12] R. Kitaura, R. Matsuda, Y. Kubota, S. Kitagawa, M. Takata, T. C. Kobayashi, M. Suzuki, *J. Phys. Chem. B* **2005**, *109*, 23378 – 23385.
[13] M. Takata, E. Nishibori, K. Kato, Y. Kubota, Y. Kuroiwa, M. Sakata, *Adv. X-ray Anal.* **2002**, *45*, 377 – 384.

